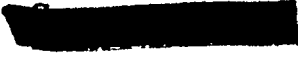




CIC-14 REPORT COLLECTION  
REPRODUCTION  
COPY

LA-2029

 0.3

AEC RESEARCH AND DEVELOPMENT REPORT

PUBLICLY RELEASABLE

Per MARK M. JONES FSS-16 Date: 7-28-95  
By longasb/DB CIC-14 Date: 1-9-96

LOS ALAMOS SCIENTIFIC LABORATORY  
OF THE UNIVERSITY OF CALIFORNIA • LOS ALAMOS NEW MEXICO

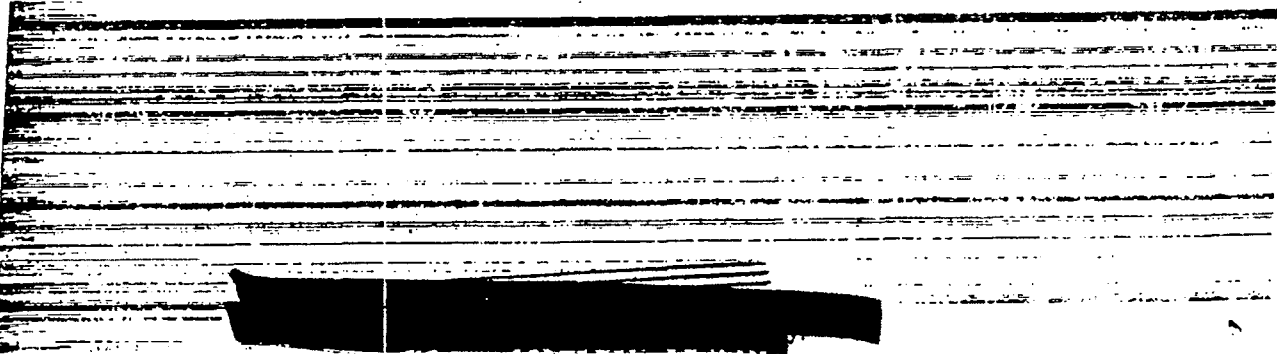
IS-4 REPORT SECTION

REPRODUCTION  
COPY

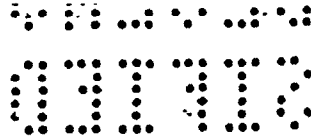
UNCLASSIFIED

TIME BEHAVIOR OF GODIVA THROUGH PROMPT CRITICAL

LOS ALAMOS NATIONAL LABORATORY  
  
3 9338 00339 4680



UNCLASSIFIED



This report was prepared as a scientific account of Government-sponsored work. Neither the United States, nor the Commission, nor any person or contractor acting on behalf of the Commission, makes any warranty or representation, express or implied, with respect to the accuracy, completeness or usefulness of the information contained in this report, or that the use of any information, apparatus, method or process disclosed in this report may not infringe privately owned rights. The Commission assumes no liability with respect to the use of, or for damages resulting from the use of any information, apparatus, method or process disclosed in this report.

Printed in USA. Charge 40 cents. Available from the U. S. Atomic Energy Commission, Technical Information Extension, P. O. Box 1001, Oak Ridge, Tennessee. Please direct to the same address inquiries covering the procurement of other classified AEC reports.

UNCLASSIFIED

UNCLASSIFIED

UNIVERSITY OF CALIFORNIA

LOS ALAMOS SCIENTIFIC LABORATORY  
(CONTRACT W-7405-ENG-36)  
P. O. Box 1663  
LOS ALAMOS, NEW MEXICO

IN REPLY  
REFER TO:

August 15, 1960

To: Copyholders of Report LA-2029

From: Report Library

Subject: ERRATA TO LA-2029

Please make the following corrections in the above report:

Page 11, last line should read,

U-235 and a diameter of about 6-3/4 in.

Page 29, Fig. 12, abscissa should read,



[REDACTED] UNCLASSIFIED  
SECRET

LA-2029  
REACTORS--RESEARCH AND TESTING  
(Distributed according to  
M-3679, 17th edition)

This document consists of 36 pages

LOS ALAMOS SCIENTIFIC LABORATORY  
OF THE UNIVERSITY OF CALIFORNIA LOS ALAMOS NEW MEXICO

REPORT WRITTEN: April, 1956 1956  
REPORT DISTRIBUTED: MAY 1

This document does NOT contain  
information subject to Section 148  
of the Atomic Energy Act.  
E. M. Sandover  
AUG 29 1989  
Date

TIME BEHAVIOR OF GODIVA THROUGH PROMPT CRITICAL

Work done by:

- L. B. Engle
  - G. A. Graves
  - G. R. Keepin, Jr.
  - J. D. Orndoff
  - T. F. Wimett
- and others in Group N-2

Report written by:

T. F. Wimett

Classification changed to UNCLASSIFIED  
by authority of the U. S. Atomic Energy Commission,

Per Jack H. Kahn 4-2-57

By REPORT LIBRARY V. Martinez  
4-19-57

Contract W-7405-ENG. 36 with the U. S. Atomic Energy Commission

LOS ALAMOS NATL. LAB. LIBS.  
3 9338 00339 4680

[REDACTED]

SECRET  
APPROVED FOR PUBLIC RELEASE

UNCLASSIFIED

UNCLASSIFIED

UNCLASSIFIED [REDACTED]

03713

!

?

UNCLASSIFIED

03713

UNCLASSIFIED

UNCLASSIFIED

SECRET

UNCLASSIFIED

## ABSTRACT

Studies were made of the time behavior of a bare spherical U-235 metal assembly (Godiva) following sudden increases in reactivity with essentially zero initial power level and no external neutron source. The highest final reactivity attained under controlled conditions was about 10 cents above prompt critical. In the region above prompt critical the observed fission rate increased exponentially until the decreasing reactivity from thermal expansion caused it to pass through a bell-shaped maximum or "burst." Following this burst, the fission rate dropped to a low-amplitude "tail" sustained by delayed neutrons and finally terminated upon automatic scrambling of the assembly. Burst amplitudes corresponding to instantaneous power levels of 10,000 Mw were observed with durations under a millisecond. Excellent agreement was found between measured reactor periods and calculations based on recent delayed neutron data. Over-all burst behavior also was found to agree with theory based on a space independent one-group model.

## INTRODUCTION

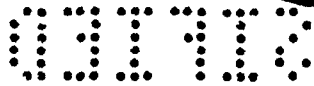
The transition region between short, but controlled, pile periods and uncontrolled, highly-supercritical conditions has been investigated with an unreflected, spherical

UNCLASSIFIED

SECRET

UNCLASSIFIED

UNCLASSIFIED

uranium assembly (Godiva). This study was undertaken because knowledge of the behavior of supercritical systems is important in evaluation of reactor hazards and also the hazards of less standard operations involving possibly critical quantities of active material.

There was very little previous experimental data in this field and what was available applied only to much more complicated systems<sup>1</sup> than Godiva. Prompt critical conditions were attained in the "Dragon" experiment<sup>2</sup> but the hydride assembly used was not favorable for a general interpretation. Additional knowledge of a qualitative nature has come from several accidental prompt critical configurations.

Theoretical treatments of the development of supercritical configurations have been given by Fuchs<sup>3</sup> and Hansen.<sup>4</sup> Fuchs discussed the energy release; Hansen extended this work to get estimates of temperature rises, pressures produced, and maximum assembly rates permissible without mechanical failure of the components.

This paper is a discussion of experiments involving measurements of the time behavior of Godiva following sudden establishment of supercritical conditions with negligible initial neutron population. With this kind of initiation, the fission rate was found to follow smoothly a rising exponential in a very short time after the sudden change; i.e., there was negligible transient excitation to confuse the interpretation. Results of such experiments in the superprompt-critical region serve to demonstrate the automatic limiting of fission energy release by thermal expansion in a fast reactor. Although only the special case of sudden approach to criticality at negligible power level is examined, the results may be extended to more general cases by application of a general theory which satisfactorily predicts the results reported here.

## THEORY

Definitions of symbols used for the Godiva assembly:

$c_i$  = Concentration of  $i$ th group of delayed-neutron precursors.

$\tau_i$  = Mean life of  $i$ th group of precursors.

$f_i$  = Ratio of number of precursors in  $i$ th group to total prompt neutrons produced per fission.

UNCLASSIFIED


UNCLASSIFIED

## UNCLASSIFIED

- $f$  = Ratio of total number of precursors to total prompt neutrons produced per fission.  
 $\gamma_i$  = Mean relative effectiveness in producing fission of a delayed neutron of  $i$ th kind compared with a prompt neutron.  
 $\gamma$  = Mean relative effectiveness of average delayed neutron compared with a prompt neutron.  
 $a_i$  = Effective fraction of total delayed neutrons which are in  $i$ th group.  
 $n$  = Mean neutron density.  
 $\Sigma_a$  = Mean total macroscopic absorption cross section (including leakage) for prompt neutrons.  
 $\Sigma_f$  = Mean macroscopic fission cross section for prompt neutrons.  
 $v$  = Mean velocity of prompt neutrons.  
 $k_p$  = Prompt neutron multiplication factor.  
 $\nu$  = Average number of prompt neutrons produced per fission.  
 $a_p = \gamma f \nu \Sigma_f$   
 $\rho_p = k_p - 1/k_p \gamma f =$  Reactivity in dollar units measured from prompt critical.  
 $\rho_0 =$  Initial reactivity (attained by the stepwise change).  
 $F(t) =$  Total number of fissions accumulated at time  $(t)$ .  
 $T =$  Reactor period.  
 $a =$  The reciprocal of the positive pile period.

Using a space-independent one-velocity group model, the pile-kinetic equations<sup>5</sup> may be written in the following form:

$$\dot{c}_i = f_i \nu \Sigma_f v n - \frac{c_i}{\tau_i} \quad (1)$$

$$\dot{n} = (\nu \Sigma_f - \Sigma_a) v n + \sum_i \frac{\gamma_i c_i}{\tau_i} \quad (2)$$

UNCLASSIFIED

UNCLASSIFIED

UNCLASSIFIED

Integrating Eq. (1) and substituting the result into Eq. (2), one obtains,

$$\dot{n}(t) = (k_p - 1) \sum_a v n(t) + \sum_i \frac{a_i \gamma_f v \sum_f v}{\tau_i} \int_{-\infty}^t n(t') e^{-(t-t')/\tau_i} dt', \quad (3)$$

where  $k_p \equiv \nu \sum_f / \sum_a$ , and variation of  $\nu \sum_f$  with time is neglected with the justification that for present purposes only the critical reactivity region is considered, and time variation in this region is negligibly small (arising only from thermal expansion). By dividing Eq. (3) by  $a_p$ , introducing reactivity,  $\rho_p$ , and total fission rate,  $\dot{F}$ , which is directly proportional to  $n$ , one obtains,

$$\frac{\ddot{F}(t)}{a_p} = \rho_p \dot{F}(t) + \sum_i \frac{a_i}{\tau_i} \int_{-\infty}^t \dot{F}(t') e^{-(t-t')/\tau_i} dt'. \quad (4)$$

Because of the temperature rise produced in the assembly by fission energy release, there is a resulting change in reactivity which, if small, is proportional to the total fissions accumulated over a time interval which is short compared with the cooling time constant.<sup>3</sup> With a constant negative temperature coefficient of reactivity, one therefore can write for the reactivity,  $\rho_p = \rho_0 - F$ , where the unit of  $F$  is chosen as that number of fissions which produces one unit (dollar) of reactivity change. This expression applies only if there is no appreciable time lag between energy release and thermal expansion. With the above modification, Eq. (4) becomes

$$\frac{\ddot{F}}{a_p} = (\rho_0 - F) \dot{F} + \sum_i \frac{a_i}{\tau_i} \int_{-\infty}^t \dot{F}(t') e^{-(t-t')/\tau_i} dt'. \quad (5)$$

UNCLASSIFIED

## UNCLASSIFIED

Exact solutions to this equation are tedious to obtain. However, approximate solutions may be found in limited regions, of which the following are useful:

Region I.  $F(t) \ll \rho_0$

For this case it is necessary simply to solve Eq. (4) (with  $\rho_p = \rho_0$ ). A solution is  $\dot{F} = \dot{F}_0 \exp(t/T)$  where  $F_0$  and  $T$  are constants. Substituting this into Eq. (4), one obtains the following equation for  $T$  (reactor period) in terms of reactivity and delayed-neutron constants:

$$\frac{1}{\alpha_p T} = \rho_0 + \sum_i \frac{a_i T}{T + \tau_i} = (1 + \rho_0) - \sum_i \frac{a_i \tau_i}{T + \tau_i}. \quad (6)$$

From the conditions of this experiment, only the positive-period solution to Eq. (6) is of interest, since pains are taken to eliminate the transients which are governed by the negative solutions. If the mean lives of delayed neutrons are much longer than the mean life of prompt neutrons, the positive solution varies rapidly with reactivity in the neighborhood of prompt critical ( $\rho_0 = 0$ ). This region is shown plotted in Fig. 1 for Godiva, using delayed neutron data presented in Table I and  $\alpha_p = 1.03 \times 10^6 \text{ sec}^{-1}$  as obtained from an independent measurement by J. D. Orndoff of the mean decay time ( $1/\alpha_p$ ) of prompt fission chains at delayed-critical reactivity (See Refs. 6 and 7).

TABLE I.  
DELAYED-NEUTRON CONSTANTS FOR GODIVA FISSION\*

i	Mean Life ( $\tau_i$ ) (seconds)	Relative Abundance ( $a_i$ )
1	78.3	0.035
2	31.3	0.207
3	8.46	0.191
4	3.14	0.409
5	0.663	0.138
6	0.188	0.020

\* Data obtained from recent measurements by G. R. Keepin and T. F. Wimett.

UNCLASSIFIED

-7-

UNCLASSIFIED

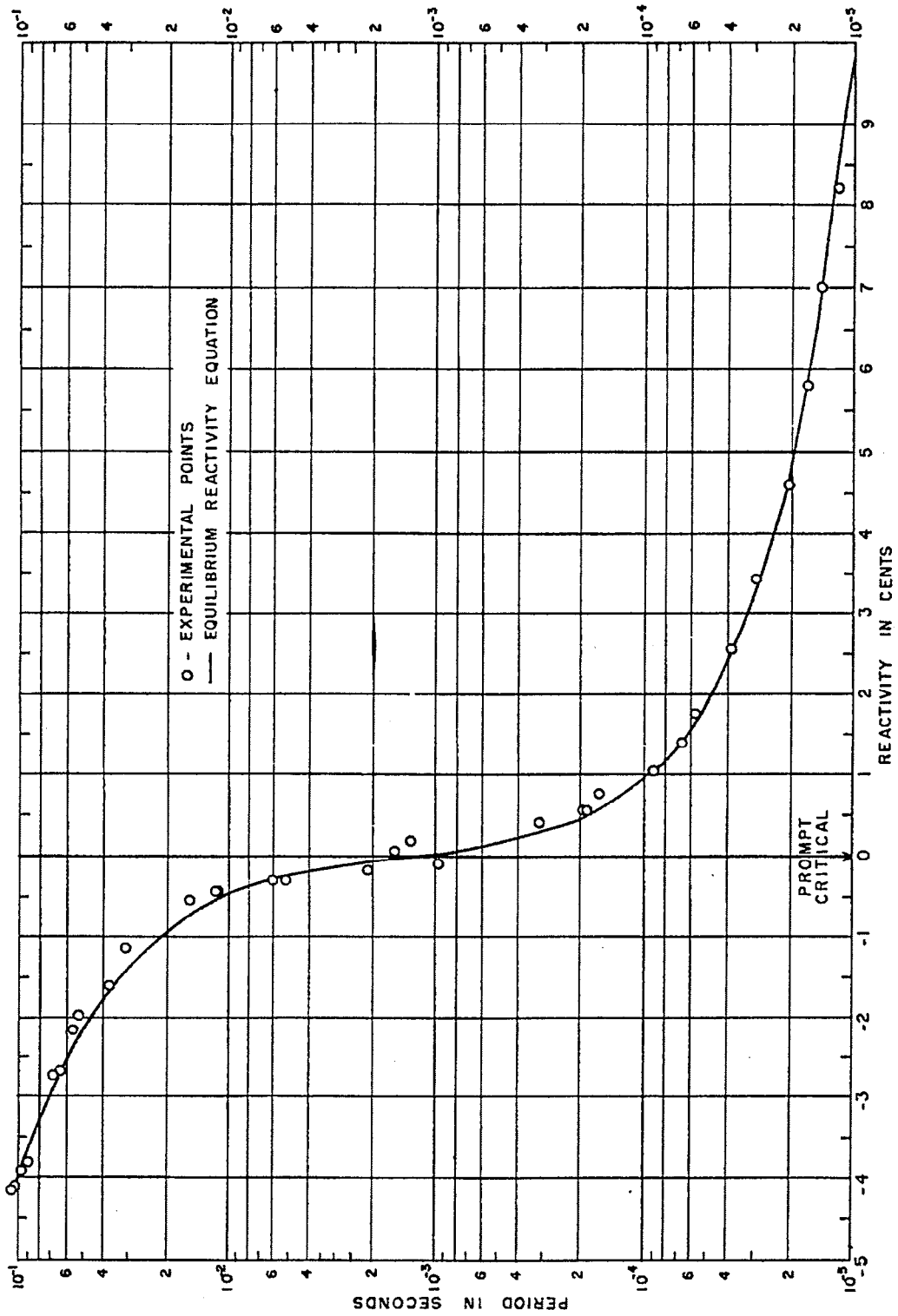


Fig. 1 Stable reactor period vs reactivity in cents measured from prompt critical.

UNCLASSIFIED

One can see a drop in the curve of Fig. 1 of over two decades in period in going from one cent below prompt critical to one cent above (1 cent = 0.01 dollar).

Region II.  $\rho_0 > 0 ; (t - t_m) \ll \tau_i$

If the boosted reactivity is in the super-prompt-critical region, the fission rate will soon break away from the pure exponential rise, mentioned above, as a result of thermal expansion and will, in fact, pass through a maximum. A solution may be obtained in this "burst" region by neglecting the delayed neutron contribution, which appears in the integral term of Eq. (5). For intense bursts, this is a good approximation; for weak ones, this would provide an approximation to prompt neutron contribution in the burst. The equation which must be solved is then:

$$\frac{\ddot{F}}{a_p} = (\rho_0 - F) \dot{F}, \quad (7)$$

which may be integrated readily to give the "burst" solutions,

$$\dot{F} = 2\rho_0^2 a_p \frac{e^{a(t-t_m)}}{\left[1 + e^{a(t-t_m)}\right]^2} \quad (8)$$

$$\text{and } F = 2\rho_0 \frac{e^{a(t-t_m)}}{1 + e^{a(t-t_m)}}, \quad (9)$$

where  $t_m$  is the time of maximum fission rate, and  $a = \rho_0 a_p$  is the reciprocal reactor period corresponding to the initial reactivity. From these equations, one obtains the following relations:

- (1) Maximum fission rate,  $\dot{F}_m = 1/2 \rho_0^2 a_p$ .
- (2) Burst width at half-maximum,  $\Delta t_{1/2} = 3.52/a$ .
- (3) Total fissions in burst,  $F_T = 2\rho_0$ .

For more intense bursts where an appreciable lag exists between energy release and volume dilation, a first order calculation yields the same equations as above except for the additional factor  $(1 + a^2\tau^2)$  where  $\tau$  is the period for a fundamental mode of mechanical oscillation of the sphere. From known values of bulk and shear moduli for uranium one obtains a value of about 10  $\mu$ sec for  $\tau$ .

Region III.  $t_m + \Delta t_{1/2} < (t - t_m) < \tau_i$

This region is that of the burst tail which was described earlier. Thus, the first term of Eq. (5),  $\ddot{F}/a_p$ , can be considered negligible since fission rate is slowly varying here, and the remaining equation may be simplified further by letting  $F = F_p + F_d$ . The first term ( $F_p$ ) or "prompt" component of  $F$  is the same as Eq. (9); the second or delayed-neutron component ( $F_d$ ) gives the burst tail. Examining first the integral term in Eq. (5), one obtains:

$$\sum_i \frac{a_i}{\tau_i} \int_{-\infty}^t e^{-(t-t')/\tau_i} \left[ \dot{F}_p(t') + \dot{F}_d(t') \right] dt'$$

$$\sim \sum_i \frac{a_i}{\tau_i} e^{-(t-t_m)/\tau_i} \left[ F_p(t) + F_d(t) + \dots \right],$$

where the integration has been performed to a first approximation. Assuming  $t > t_m + \Delta t_{1/2}$ , one obtains from Eq. (9),  $F_p(t) \sim F_T = 2\rho_0$ . With these approximations, Eq. (5) becomes

$$[F_d(t) + \rho_0] \dot{F}_d(t) \approx \sum_i \frac{a_i}{\tau_i} e^{-(t-t_m)/\tau_i} [2\rho_0 + F_d(t)]. \quad (10)$$

From Eq. (10), one immediately obtains an upper bound for  $F_d(t)$  by letting  $\rho_0 \gg F_d(t)$ . For this case (intense bursts), one finds

$$\dot{F}_d \sim 2 \sum_i \frac{a_i}{\tau_i} e^{-(t-t_m)/\tau_i} \quad \text{if } \rho_0 \gg F_d(t), \quad (11)$$

which simply represents the decay of delayed-neutron activity following an "instantaneous" fission activation of uranium. In a similar manner, one may also obtain as a lower limit in this region

$$\dot{F}_d \sim \sum_i \frac{a_i}{\tau_i} e^{-(t-t_m)/\tau_i} \quad \text{if } \rho_0 \leq 0. \quad (12)$$

More precise determination of  $\dot{F}_d$  is tedious and generally requires numerical integration.

The following is a brief discussion of stresses produced by fission bursts. Since the spatial fission distribution (zero order Bessel function of radius) has a maximum at the center of Godiva, the resulting instantaneous internal pressure is also maximum at the center and, consequently, generates pressure waves in the sphere which lead to oscillating tensions at the surface of magnitude equal roughly to the maximum central pressures. Maximum tensions as predicted in Ref. 4 are of the order of 1500 atmos for a burst which produces a temperature rise of 100°C, and a 250°C burst would exceed the 5000 atmos tensile strength of uranium. Accordingly, an upper limit of 100°C was placed on the burst temperature rises of this experiment.

#### DESCRIPTION OF APPARATUS

Lady Godiva (see Refs. 7 and 8) is a bare U-235 metal reactor which is fabricated in three sections that go together to form a sphere. Figure 2 shows Godiva in the disassembled state. The central section is fixed in position by small tubular steel supports while the upper and lower sections are retractable by means of pneumatic cylinders, thus providing two independent scram mechanisms. The completed assembly has a critical mass of about 54 kg of uranium enriched to about 90 percent isotopic abundance in U-235, and a radius of about 6-3/4 in. Godiva is operated

*DIAMETER* See attached  
Errata Sheet

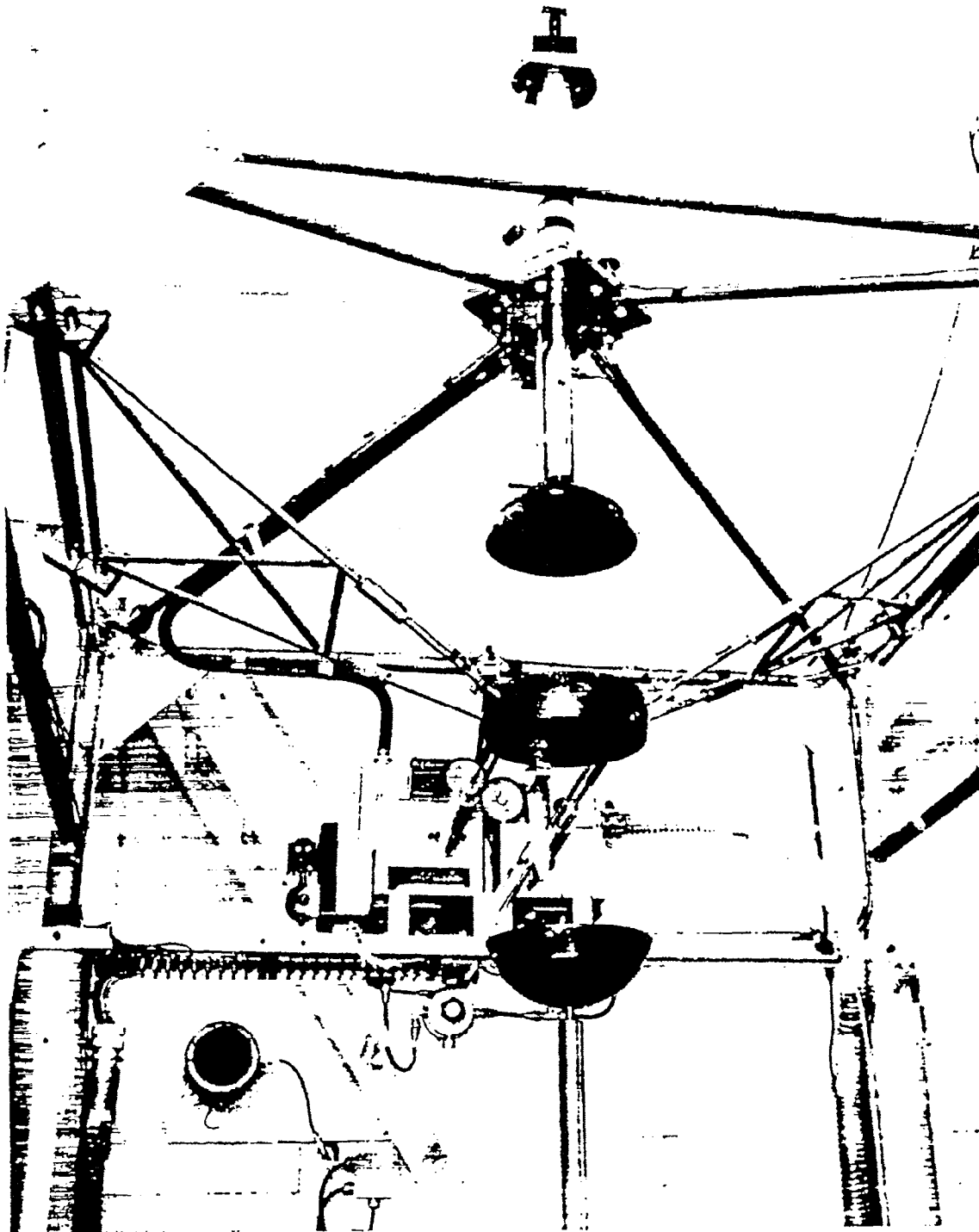


Fig. 2 View of Godiva in scrammed state showing hangar system.

remotely from a control room one-quarter of a mile away.

Stepwise reactivity adjustment is accomplished by adding small cylinders or "buttons" in some of the fourteen recesses provided on the surface of Godiva and visible in the photographs of Figs. 2 and 3. Two 7/16-inch-diameter uranium control rods which enter the central section afford continuous reactivity control with reproducibility in position to 0.001 in. or about 0.01 cent in reactivity units. The control rods together with mechanical-drive units and selsyns for indicating position at the control room can be seen in Fig. 3, where Godiva is shown in normal-uranium mockup.

Also entering the central section of Godiva is a third uranium rod about 1/2 in. in diameter which is used to provide the rapid increase in reactivity mentioned earlier. Figure 4 shows this so-called "booster slug" with an early model of the associated mechanism for rapid insertion. Initially projecting into the assembly about 2 in., the booster slug is fired by an explosive charge into a final position where 1 in. of rod protrudes from Godiva at each end. An oil dashpot is used for stopping it, and special magnetic locks connected to the driving rod serve to reduce rebound. With this insertion device, a transit time of approximately 5 msec was achieved. A later model, which is much more convenient, employs an air cylinder for both insertion and withdrawal of the booster, and yields a transit time of roughly 30 msec. Because of the very low neutron background in Godiva, there was as much as 5-sec delay between slug firing and a burst, which indicated that rapid transit of the slug was not essential.

Godiva is housed normally inside a building having thick concrete walls, but, in one phase of the present experiment, the assembly was made portable and was suspended 25 ft above the ground outdoors in an effort to eliminate room-return and ground-scattered neutrons. Figure 5 shows the setup for outdoor operation with radiation monitors and scram devices in the rack at the lower right.

## INSTRUMENTATION

Measurements of the following were made in each run of this experiment: (1) reactor period, (2) burst shape, (3) temperature rise, and (4) total fission yield. The reactor period measured was the positive period associated

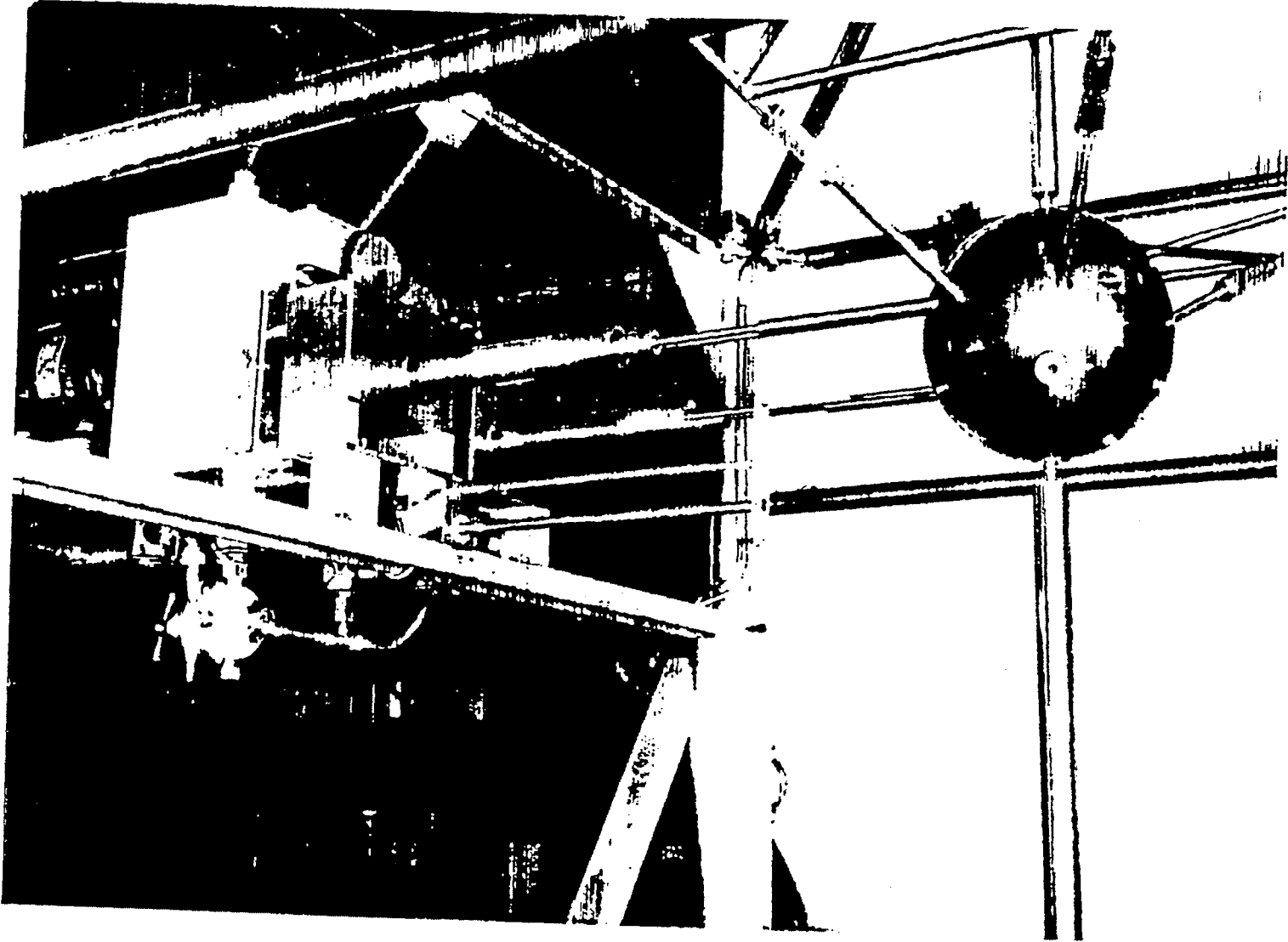
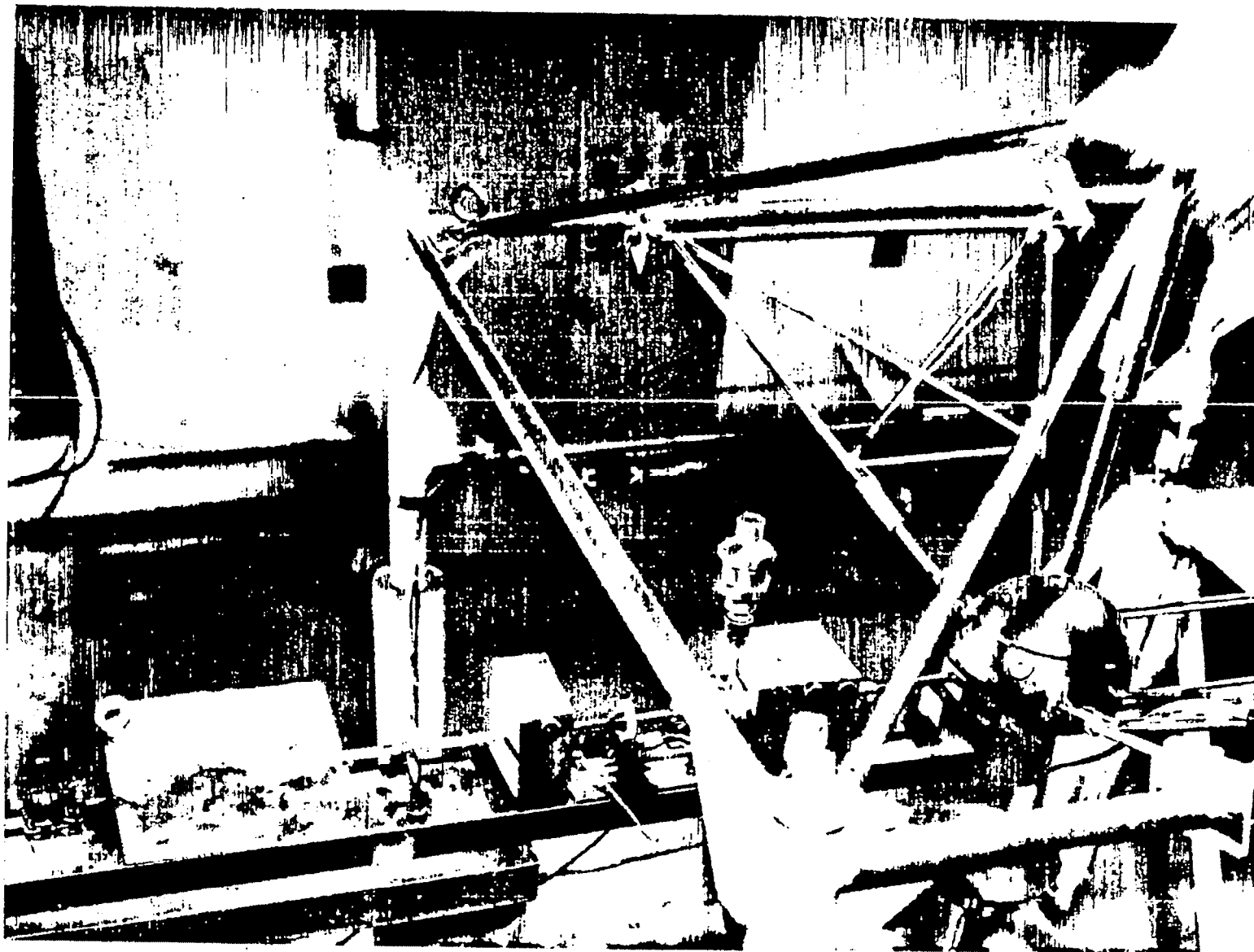


Fig. 3 Godiva assembled in normal-U mockup with control rods and drive units visible at the left.



-15-

Fig. 4 Reactivity booster system attached to Godiva. From left to right, solenoid for firing blank cartridge, firing chamber, magnetic stops, oil dashpot, uranium booster rod, and Godiva partially assembled.

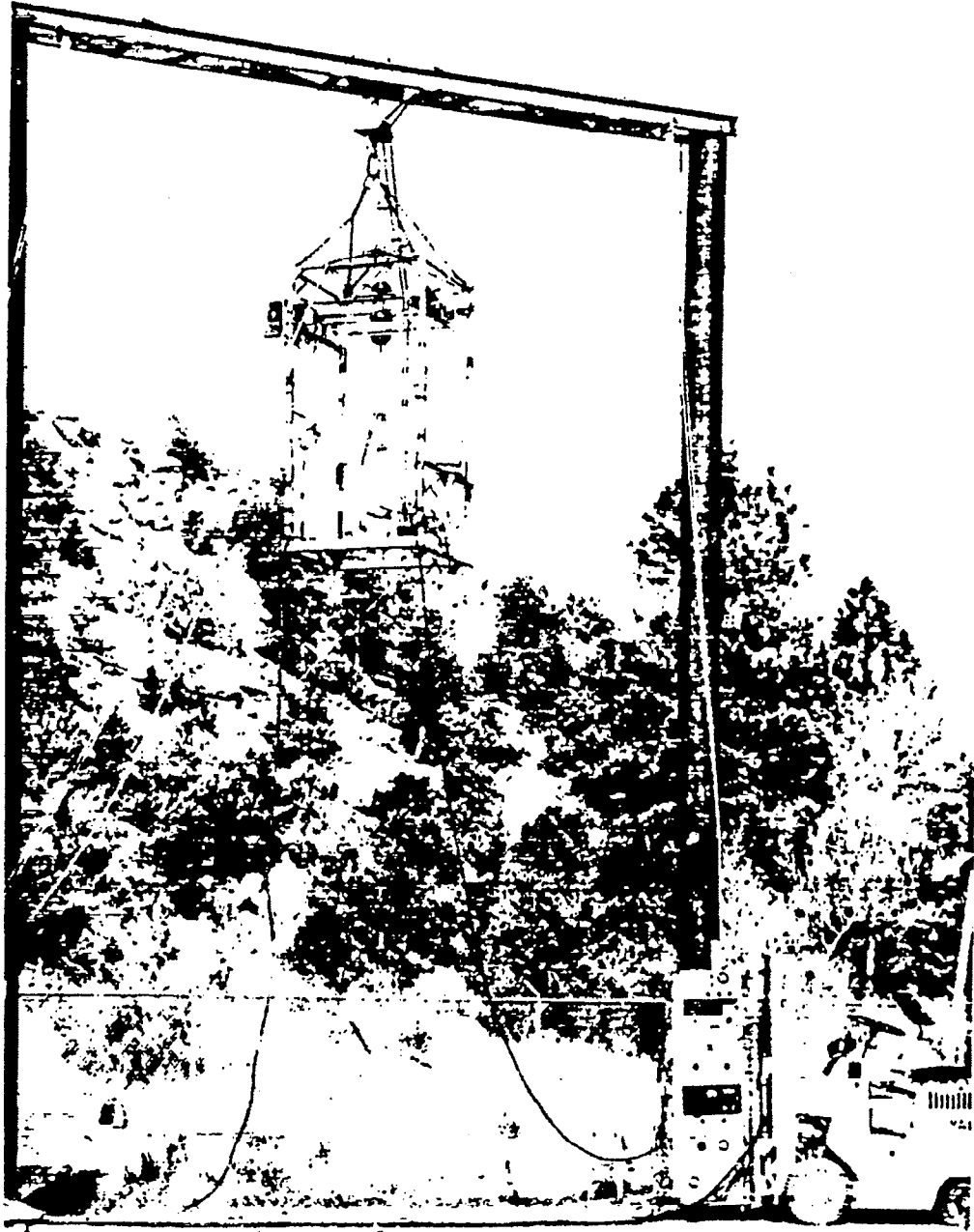


Fig. 5 Godiva suspended for outdoor operation.

with the early part of the rise in fission rate. Burst shape was obtained by observing the leakage flux as a function of time. Temperature rise refers to the increase in mean temperature of the assembly resulting from fission energy release, or total fission yield, the measurement of which will be discussed later.

An RCA 5819 scintillation counter with a liquid organic phosphor (DPT) constituted the primary flux-sensitive device for the measurement of reactor period. The counter was mounted on the framework supporting Godiva, and the output was partially integrated and coupled through a cathode follower circuit to a coaxial transmission line terminated at the control room, where the output voltage was applied to the horizontal deflection plates of an oscilloscope. An increasing flux would thereby cause the beam to deflect across the oscilloscope face where time markers were supplied by sine waves of known frequency applied to the vertical deflection plates. The trace so obtained was automatically photographed and the period extracted by analysis of the negative. A typical photograph of such a trace is shown in Fig. 6, together with a plot of the logarithm of deflection vs time, the slope of which yields the period. Throughout these measurements, two essentially identical, but independent, detector-oscilloscope systems were employed which differed by about a factor of ten in over-all sensitivity. This permitted the observation of the power-level rise over about two decades and provided two independent determinations of initial period for each burst. The two values so-obtained agreed to within  $\pm 5$  percent for all bursts reported here.

For studying the over-all burst shape, where power levels of interest extended over four decades, a special high-current photocell (RCA C7154) was employed with 3 gal of liquid scintillator as the flux sensitive material. The scintillator (diphenylhexatriene in a saturated solution of terphenyl in toluene) responded to both gamma and neutron radiation. In the region of operation, the anode current of the RCA C7154 was linear from zero to 20 amp. The container for this counter was also mounted on the Godiva framework and may be seen in Fig. 5. Output current from this counter was fed into a 400-ohm resistor in the control room where the voltage across it was applied to the vertical amplifiers of four oscilloscopes in parallel, each one equipped with a camera with automatic shutter. Linear horizontal sweeps of different sweep rates combined with different vertical amplifications in the oscilloscopes served to provide a complete record of a burst over three decades

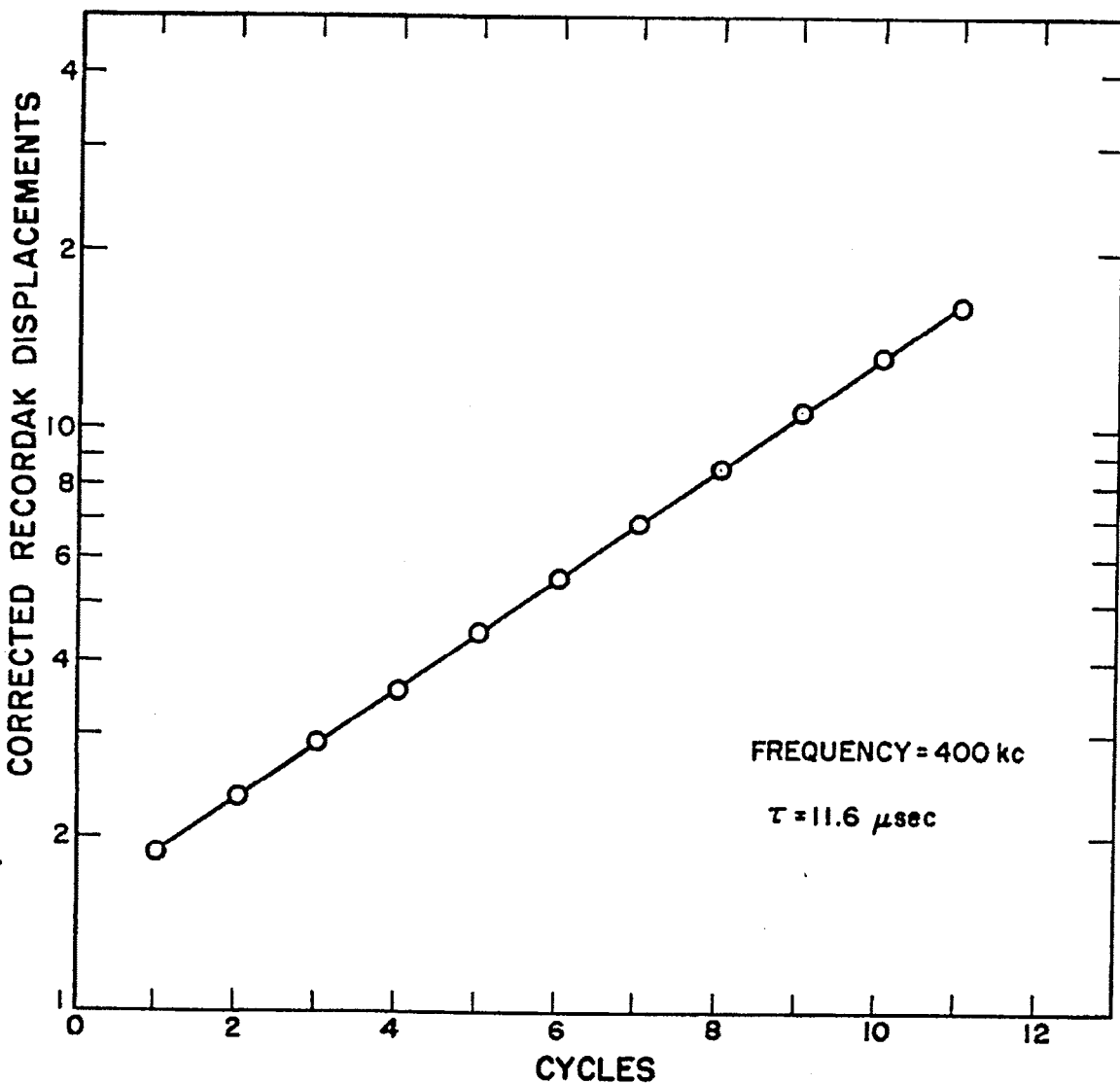
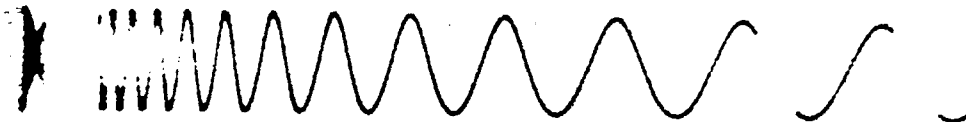


Fig. 6 Photograph of scope trace for positive period measurement with plot of horizontal deflection (power level) as read on Recordak film reader vs time using sine wave time markers. Slope of the curve gives positive period.

in time and four in amplitude. Special amplitude clipping circuits prevented saturation of the high-gain amplifiers. Triggering of the camera shutters and oscilloscope sweeps was effected by a voltage pulse generated by a third scintillation counter circuit at the instant the incident flux from Godiva exceeded a predetermined level.

The radiation-level trigger was used also to trip the scram circuits which automatically retracted the upper and lower sections of Godiva. Because of electrical delays in the circuit, the actual scrambling took place about 40 msec after trigger time; this allowed sufficient time to observe and record burst shapes, etc., yet was fast enough to prevent unnecessary heating of Godiva. One exception will be mentioned later where a slower scram device was employed, allowing a scram delay of about 0.4 sec.

An iron-constantan thermocouple attached to one of the control rods, which was set always at its innermost position during a burst, was used to measure assembly temperature. The calibrated output was presented on a Brown Recorder so that initial temperature could be observed together with the cooling curve following a burst. The thermocouple was located about 2-1/2 in. from the center of the sphere which is the radial position of mean fission density, hence mean temperature rise. To correct for cooling, an extrapolation was made on the recorded cooling curve back to burst time. A further complication was introduced by the fact that the assembly was automatically scrambled before the thermal energy became uniformly distributed throughout the sphere by conduction. The central section, therefore, was left with more than its share of heat. It was found, however, that application of a small theoretical correction (discussed later) to the mean temperature as measured in the middle section yielded results which were accurate to about 1 percent.

Fission yield for each run was obtained by measuring the (n,p) induced activity of a compressed sulfur pellet attached to the surface of Godiva. Sulfur pellet activation was related to total fissions in the assembly by calibration against a radiochemical determination (by J. E. Sattizahn and others in Group J-11) of total fissions per gram obtained in a uranium sample irradiated at the center of the assembly. The ratio between total fissions in Godiva and central fission density was calculated from the measured normal spatial flux distribution.

Since a primary reference variable in all runs was reactivity, some measurement of this quantity was essential. A convenient unit, whose absolute evaluation was

necessarily delayed until completion of the experiment, was the "linear control rod inch" (LCRI). Changes in control rod position were reduced to LCRI by application of a control-rod-effectiveness correction curve.<sup>7</sup> The procedure followed in a run was to find the correct control rod position for delayed critical operation with the booster slug out. Firing of the booster slug would then boost reactivity to a point near prompt critical which was thus established as a fiducial. In practice, the upper section of Godiva was retracted after the delayed-critical determination was completed in order to allow neutron activity to decay. Allowing 1/2 hr for this, the control rod then was set at a known (LCRI) distance away from the fiducial position, the upper section lowered, and the booster slug fired before an appreciable neutron population could build up.

Calibration of LCRI in terms of reactivity units was done in several ways, the most precise of which was the direct evaluation of the increment between delayed and prompt critical (1 dollar) in LCRI units. The location of prompt critical was determined in the course of this experiment and will be described in the next section.

#### EXPERIMENTAL RESULTS

Measurements of positive period are shown plotted against reactivity on the graph of Fig. 1. Actually, the primary measurements of period were made against LCRI units, but to facilitate comparison with theory, points here were plotted against cents by making use of the conversion from LCRI to reactivity units mentioned in the preceding section. Very good agreement between measured periods and the theoretical curve obtained from delayed neutron data can be seen. A further comparison between these data and theory can be made by referring to Fig. 7, where reciprocal period is plotted against reactivity. It was by utilizing this kind of plot with reactivity measured in LCRI measured from the before-mentioned fiducial that prompt critical was precisely located. Prompt critical is defined here as the intercept on the abscissa of a straight line through the data (since in this region delayed neutron contribution to period is negligible). The slope of such a line is  $\alpha_p$  according to Eq. (6). The curve in Fig. 7 was drawn with a slope of  $1.03 \times 10^6 \text{ sec}^{-1}$  per dollar, the value obtained independently for  $\alpha_p$  as discussed earlier. Again, one finds the

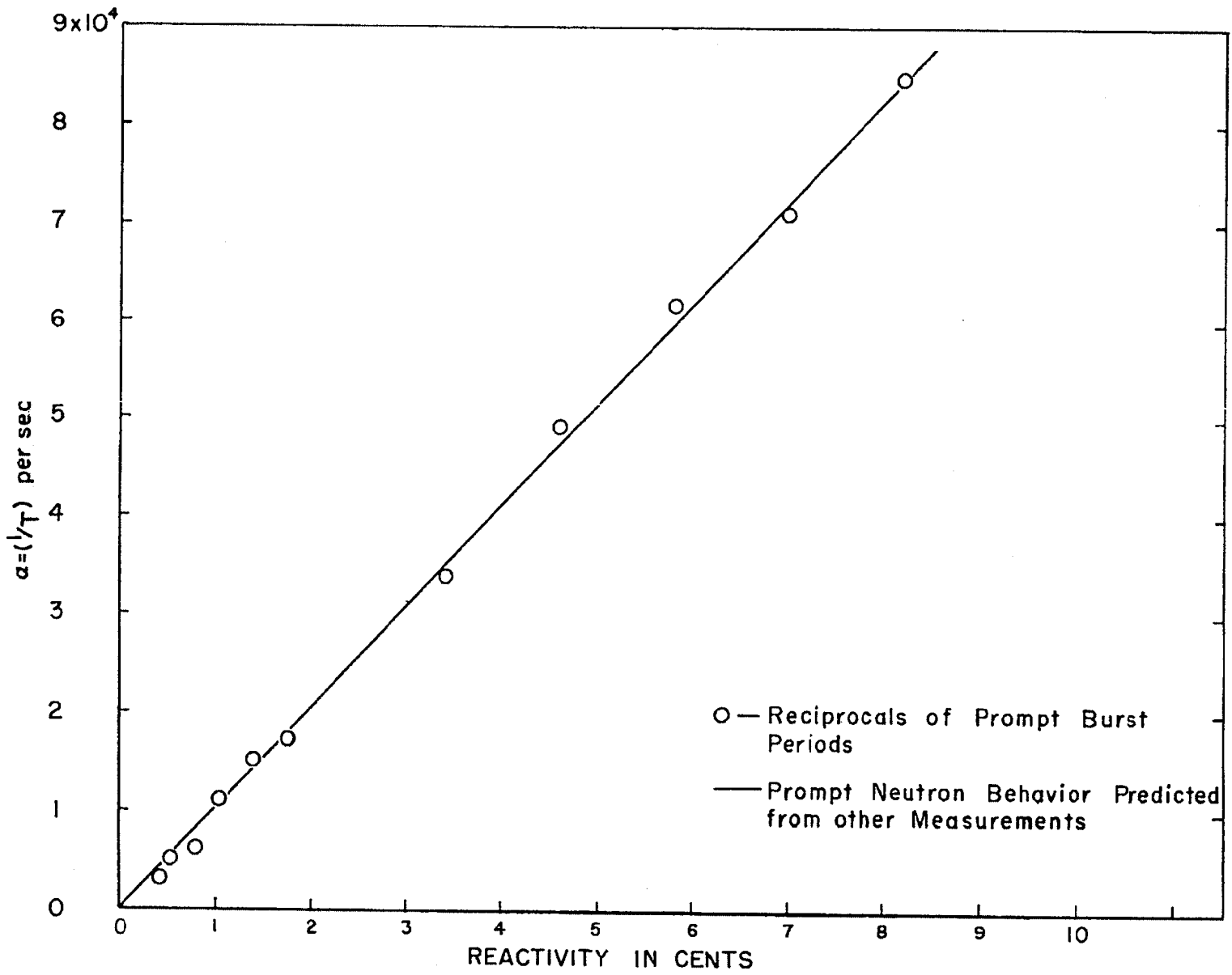


Fig. 7 Plot of reciprocal reactor period vs reactivity.

data in good agreement with theory. The fact that the data match theory at the inversion point of Fig. 1 results, of course, directly from the above extrapolation for finding prompt critical, but the match away from prompt critical and, in particular, the slope agreement above prompt critical in Fig. 7 constitute an independent check with theory.

Just how critical the above slope agreement is may be demonstrated by an early discrepancy when indoor data were used for the plot of Fig. 7. The slope of the best straight-line fit to that data was  $0.94 \times 10^6 \text{ sec}^{-1}$ . This apparent disagreement with the known value of  $\alpha_p$  was finally resolved by recognizing the existence of an effective delayed neutron group in the millisecond region resulting from room-return neutrons and amounting to about 2 percent of total delayed neutrons.

Some typical photographs of oscilloscope traces of burst shapes are shown in Fig. 8. Appropriate time scales and reactor periods are shown below each photograph, and vertical deflection sensitivities in terms of fissions per second are indicated at the right. Calibration of the phototube output in terms of fission rate was accomplished by measuring the entire time-voltage integral of a burst trace up to the scram point and equating it to the total number of fissions as determined by the sulfur-pellet fission monitor. This calibration was made for each run because there was an unexplained gain variation of about a factor of 2 in the burst detector system. The trace at the upper left illustrates sub-prompt-critical self limiting; the one to the right of it shows the bell-shaped burst just beginning to emerge; the central trace shows an intermediate burst with the residual tail still prominent; the bottom two traces show a well-developed intense burst with the tail on the left and the burst proper, which is photographed with very much less vertical amplification, at the right. An interesting feature of this burst is that it demonstrates the "bounce-effect" wherein pressure waves in the sphere cause the upper sphere component, which is seated by gravity, to bounce as much as a half inch, thus momentarily reducing the reactivity below critical. This effect is seen as a drop in amplitude near the beginning of the trace at the lower left with subsequent reassembly appearing as the restoration of the residual level in about 0.1 sec. The superposed sine waves are double exposures introduced for both amplitude and time calibration of the oscillographs.

Complete bursts are shown plotted against logarithmic coordinates in Fig. 9. The more intense of these bursts were plotted piecewise from four different photographs as

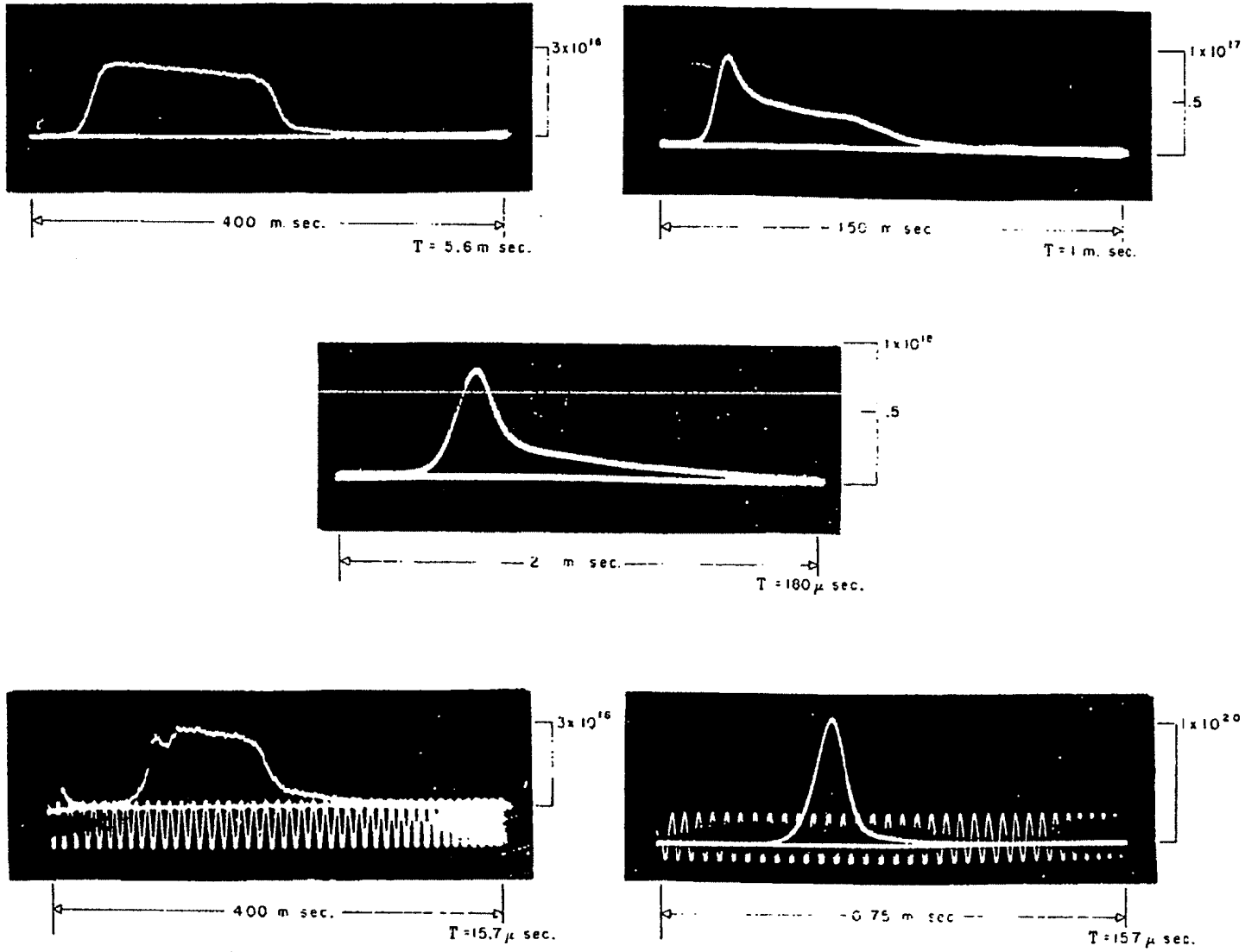


Fig. 8 Typical burst photographs.

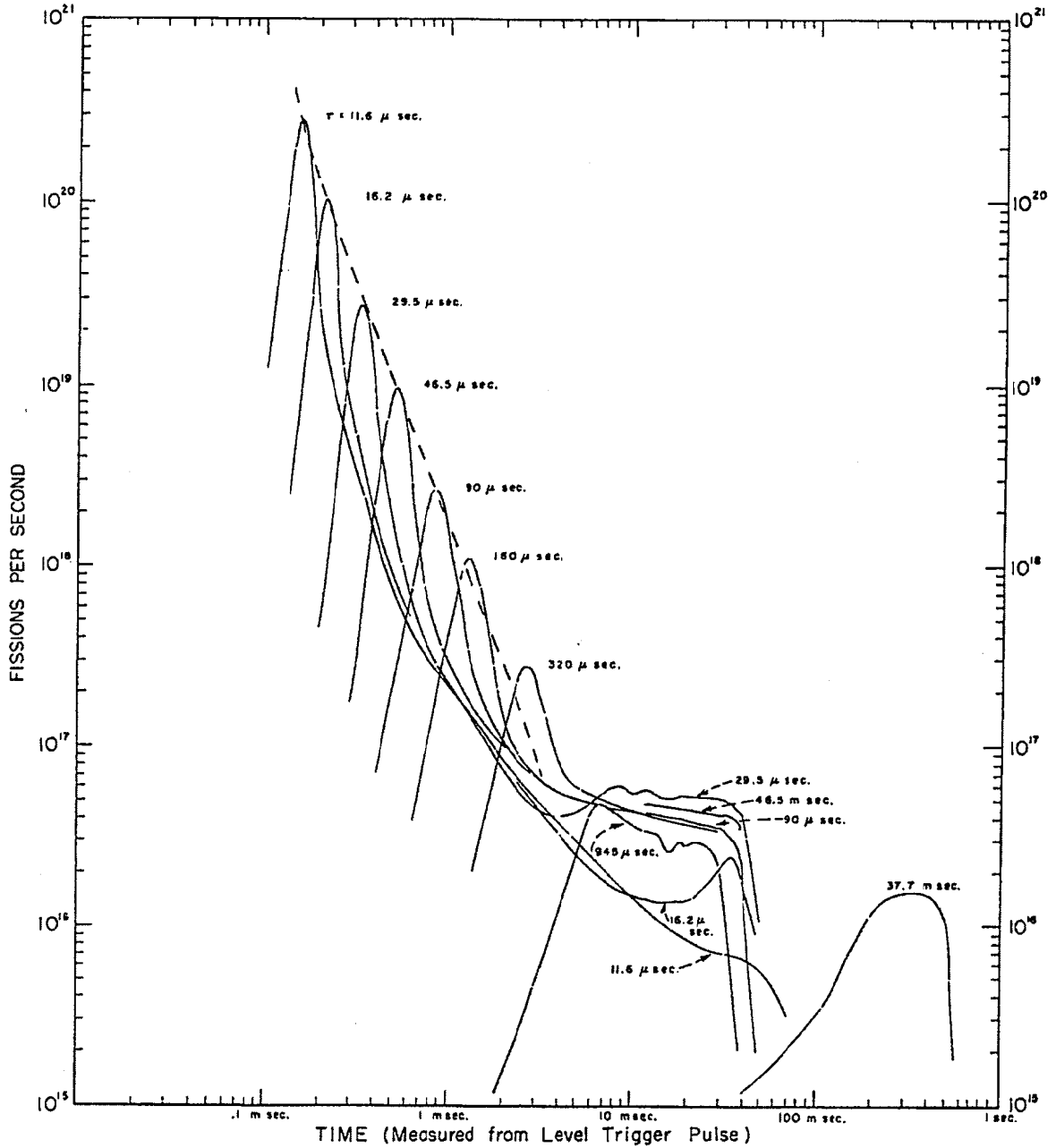


Fig. 9 Plots of complete bursts taken from photographs as in Fig. 8.

described earlier. For convenience, time was measured from level-trigger time and all bursts terminate at about 35 msec with the one exception shown, namely, the sub-prompt-critical "burst" with  $T = 37.7$  msec. For this run, scrambling was delayed to allow time for development of the burst. The dotted curve passing through the peaks is a calculated curve showing position of peaks if the trigger occurred at the same amplitude for all bursts. Because of smoothing circuits in the trigger generator, this wasn't always the case, and weaker bursts experience more than the predicted delay. The plots of Fig. 9 also exhibit the interesting feature that all bursts appear with roughly equal widths on the scale used. Evidence of the bouncing discussed earlier can be seen in the tails of the three most intense bursts. All bursts shown in the figure were produced outdoors.

Two of the bursts of Fig. 9 are shown in Fig. 10 with calculated curves superposed for comparison. Equation (8) was used for the early part of the calculated curves and a second-order theory (too lengthy to present here) for the residual level or tail. Also appearing on the graph are the limits as predicted by Eqs. 11 and 12. Good qualitative agreement can be seen between theory and experiment although there exists a general amplitude discrepancy at low levels.

Since the theory is given in terms of dollars and the experimental results of Fig. 10 in terms of fissions, a conversion had to be introduced from dollars to fissions. This was done by combining two temperature coefficients. The first was the temperature coefficient of reactivity, which was obtained from a quasi-static measurement of the LCRI change with temperature ( $0.035$  LCRI/ $^{\circ}$ C) for constant reactivity and multiplying by the conversion factor  $0.1196$   $\$/$ LCRI to give  $0.0042$   $\$/$  $^{\circ}$ C. The second coefficient was the number of fissions required to raise the temperature of Godiva one degree. This could be calculated from the average energy released per fission and the total heat capacity of the assembly. However, since the burst detector was calibrated in terms of fission rate as determined radiochemically, it was decided to employ a direct measurement of average fission yield per degree temperature rise as measured in the central section. Figure 11 shows a plot of fission yield vs temperature rise for two sets of data, and a calculated curve is also shown for comparison. The data for the lower curve were obtained after an accident (to be discussed later) which warped Godiva and necessitated the addition of over a kilogram of uranium. In addition, a slightly different procedure was used for these data to derive fissions from the sulfur pellet and probably accounts

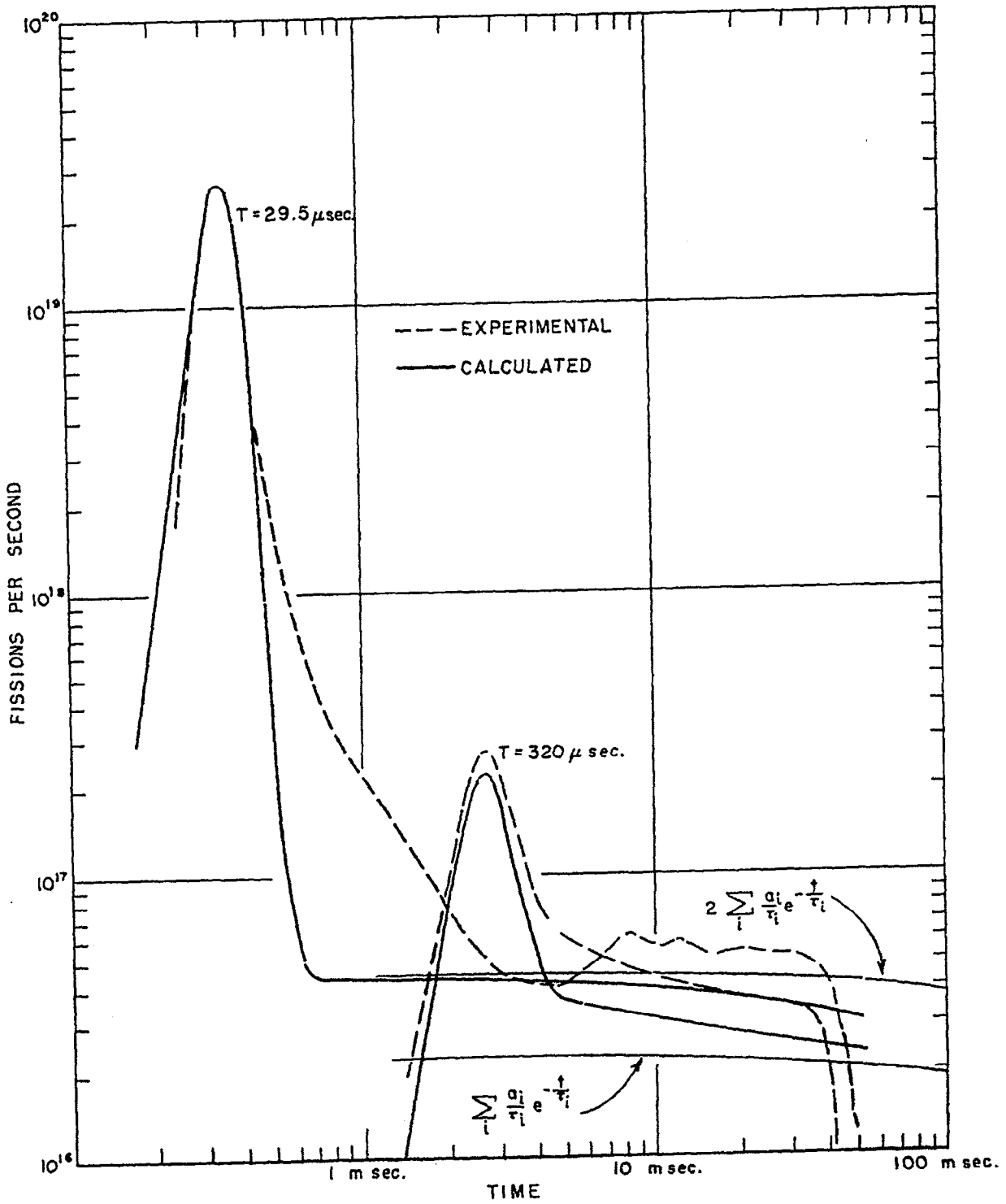


Fig. 10 Comparison of two experimental bursts with first order theory.

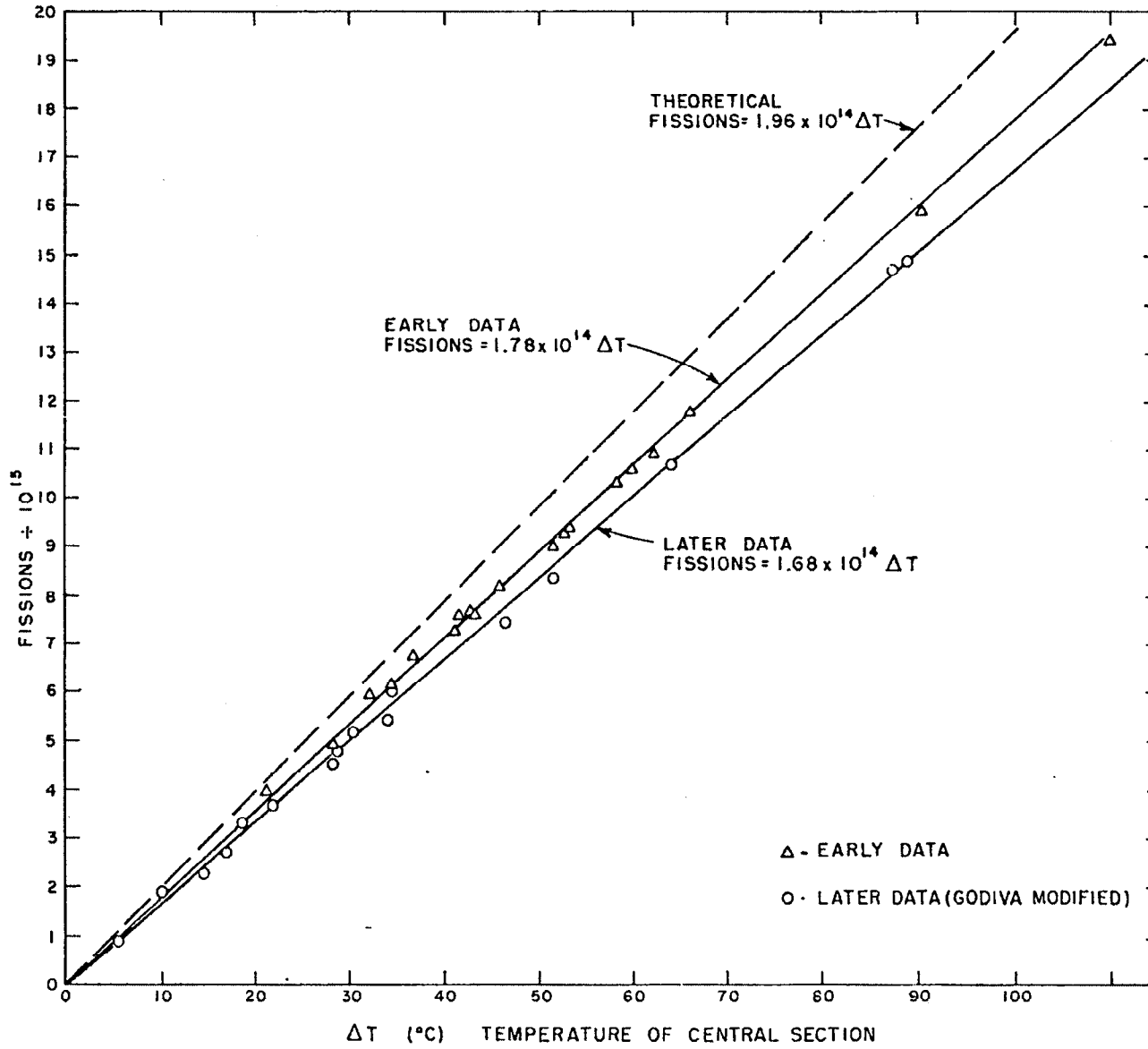


Fig. 11 Total fission yield vs temperature rise in central section.

for the observed difference of about 5 percent between the two sets of data.

The ratio of the temperature of the insulated central section to what it would be if the heat energy were allowed to become uniformly distributed throughout the complete assembly was calculated from volume integrations of the known spatial fission distribution. For the repaired assembly (which was used for the bursts of Fig. 10), this ratio was found to be about 1.2. The calculated curve was obtained by using this result, 0.0287 cal/°C for the specific heat, 55,460 grams for the prompt-critical mass and a presumed 178 Mev of heat energy imparted to the assembly per average fission to give  $1.96 \times 10^{14}$  fissions per degree rise of the central section. Agreement between this curve and either set of data is rather poor even though the slope is practically independent of the assembly configuration change. Using the slope of the lower curve which applies to the bursts considered, the over-all temperature coefficient of fission becomes  $1.2 \times 1.68 \times 10^{14} = 2.02 \times 10^{14}$  fissions per degree change in the complete assembly. Finally, dividing this by the temperature coefficient of reactivity yields  $4.8 \times 10^{16}$  fissions per dollar.

Variation of measured burst characteristics with positive period is shown plotted in Figs. 12, 13 and 14. Reactor period was chosen here as the independent variable rather than reactivity, because the period measurement was found to provide a more precise determination of reactivity than control-rod position. The straight line through the data of Fig. 12 is the best square-law fit to the data in agreement with a prediction ( $\dot{F}_m = a^2/2a_p$ ) derived from Eq. (8). Because of the lag between fission energy release and volume expansion for short periods, more intense bursts are obtained than are predicted by Eq. (8), with the increase given to a first approximation by the added inertial factor  $(1 + a^2\tau^2)$ . The curved line of Fig. 12 was calculated using this factor with  $\tau = 9 \mu\text{sec}$  and is in good accord with the data.

Figure 13 shows burst yield plotted against reciprocal period. Fission yield refers to fissions in the early part of the burst or "spike" and was obtained from graphical integration under that part. The region of interest was plotted on linear paper and the area cut out and weighed on a balance. It will be noted that fission yield is linear with period only at low values. The straight line is calculated from Eqs. (8) and (9) with peak fission rate taken

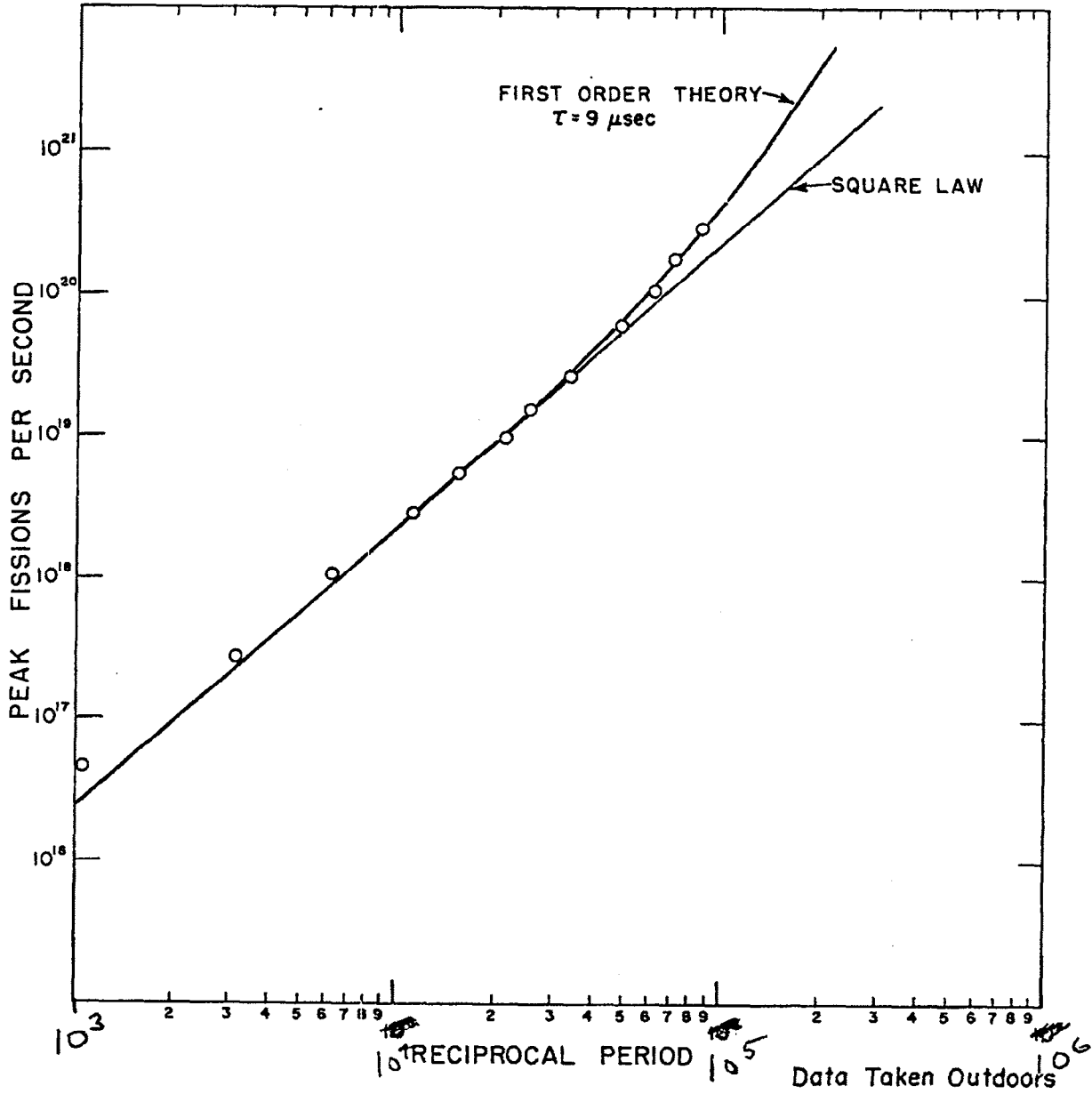


Fig. 12 Peak fission rate vs reciprocal initial reactor period.

See attached  
Errata Sheet

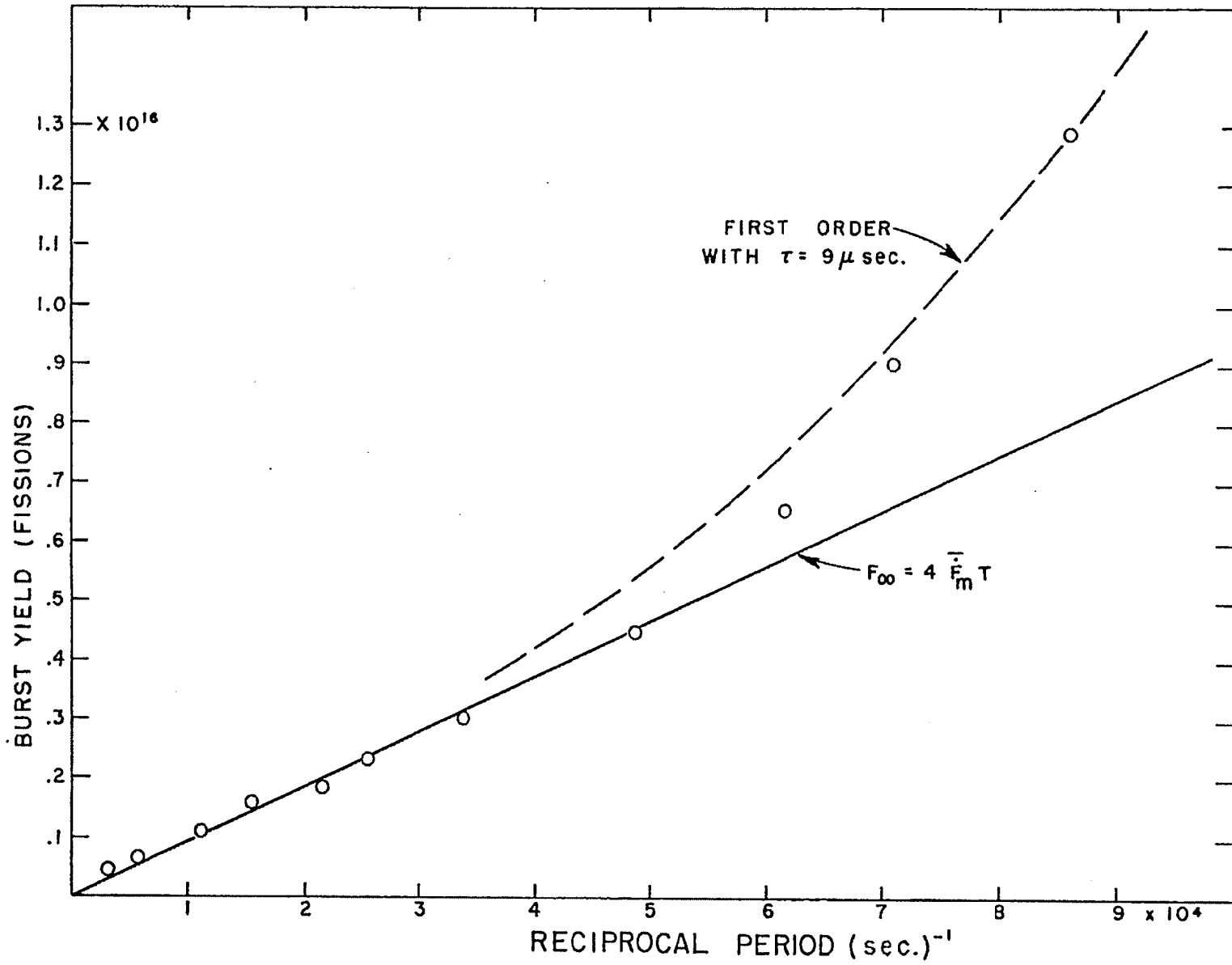


Fig. 13 Fission yield vs reciprocal initial reactor period.

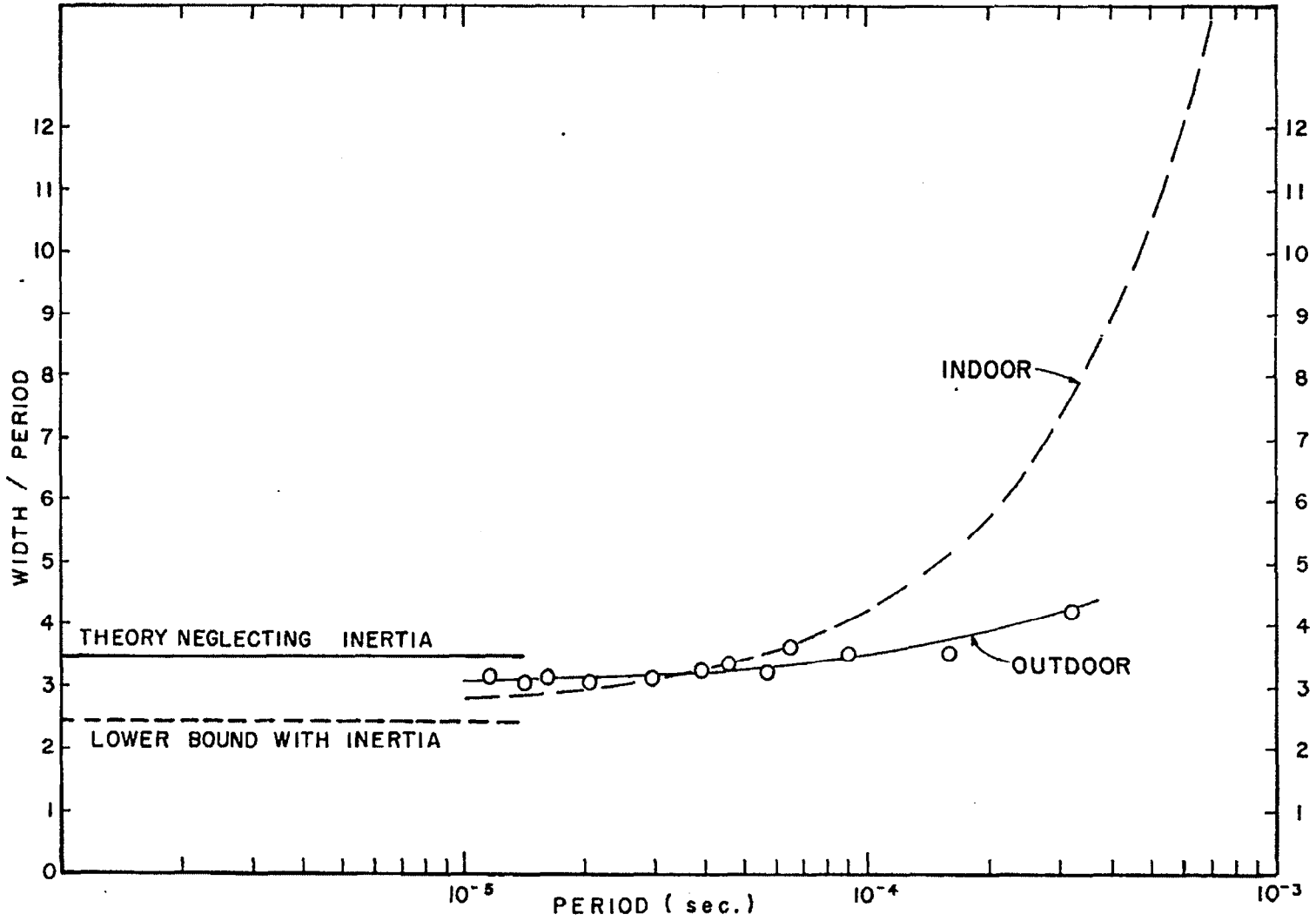


Fig. 14 Variation of burst width with period.

from the straight line of Fig. 12. Again, agreement is improved by resorting to the inertial approximation at higher yields. However, the data seem to break away from the linear curve even faster than predicted by the corrected theory.

Figure 14 shows the variation of burst width at half maximum with period. The prediction of Eq. (8) is indicated by the upper straight line. The solid line through the data was drawn as the best fit to the data which were taken outdoors. The dashed line shows the corresponding behavior of indoor data.

As noted on page 22, the effect of room scattering on the behavior of Godiva is believed to be represented satisfactorily by additional delayed neutrons in the millisecond region. This conclusion was drawn, in part, from evidence such as is illustrated in Fig. 15 where the 320  $\mu$ sec outdoor burst is drawn superposed on an equivalent indoor burst. To aid in detailed shape comparison, the bursts are normalized to unit peak amplitude, and time is plotted in units of reactor period. More area is observed under the trailing edge of the indoor burst than the outdoor one after the peak, but the difference between the two is found to decrease with a decay time of a few milliseconds. By means of a numerical solution to Eq. (5), L. B. Engle has found that the addition of equal parts of 1-msec and 10-msec groups to the normal delayed neutrons does indeed result in a calculated trailing edge which satisfactorily matches that of the indoor burst. The total relative abundance required for the added groups was about 0.015, or 1-1/2 percent of all delayed neutrons. In order to account for an apparent increase in reactivity contributed by the room in delayed-critical operation, additional room-return neutrons must be postulated amounting to about another 1 percent of total delayed neutrons. If these had mean lives of less than a millisecond, they would be indistinguishable from prompt neutrons in their effect on burst shape.

In all Godiva experiments, operation of the assembly is in strict accordance with detailed safety regulations and, in addition, various interlocks are incorporated into the control circuits to eliminate the possibility of practically all foreseeable procedures which would result in damage to Godiva or personnel. Safety of personnel is virtually assured, of course, because of the remote operation. However, with the unusual requirements of the burst experiment, it was impossible to remove all possibilities of dangerous procedure by means of interlocks. Consequently, because of a combination of human errors, an extreme burst was produced accidentally in the course of this experiment

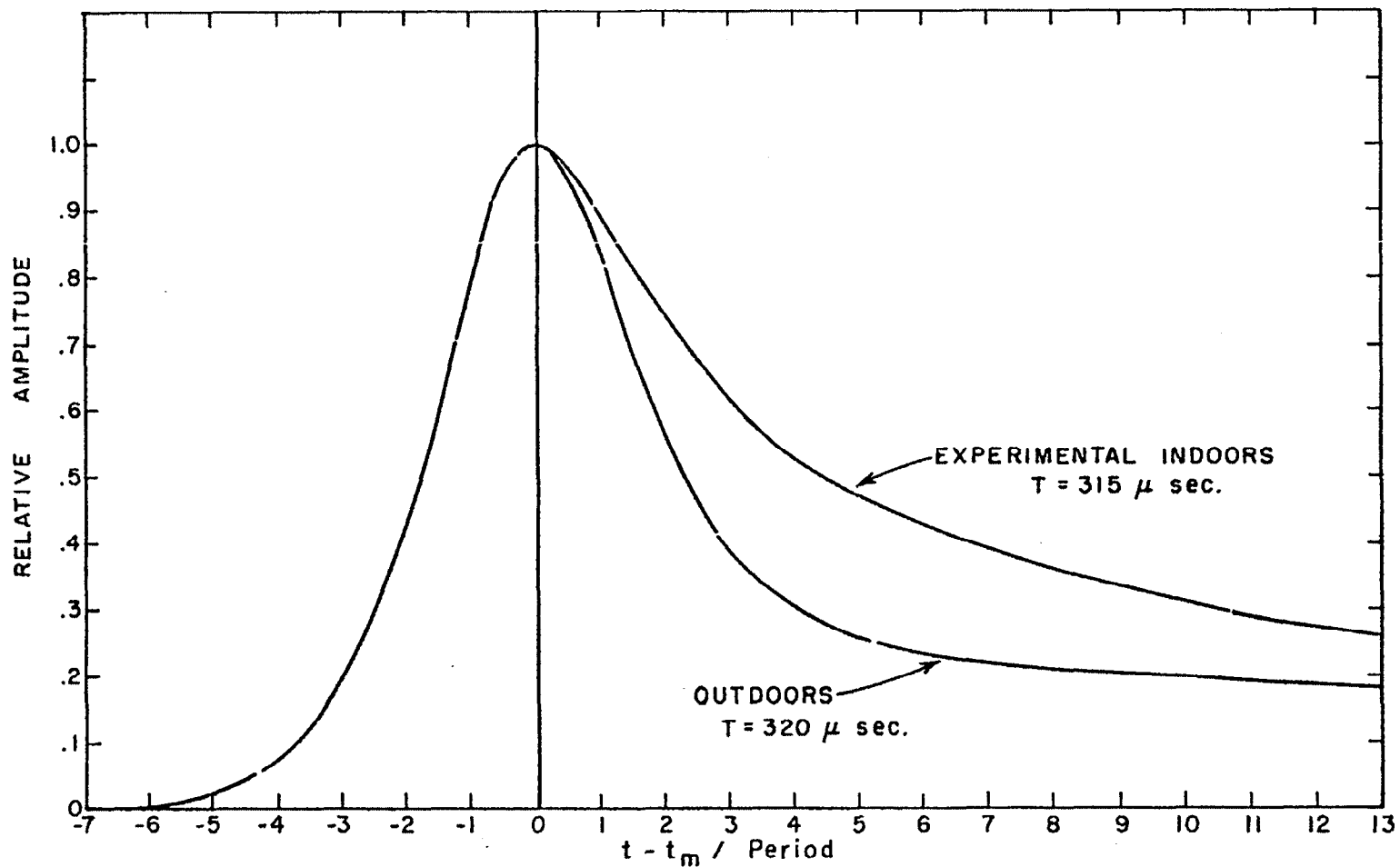


Fig. 15 Comparison of indoor and outdoor bursts.

UNCLASSIFIED

and resulted in considerable damage to the assembly, as can be seen in the photograph of Fig. 16. There was no significant loss of active material, however, and some information was gained from this burst but, unfortunately, most of the measuring instruments became saturated. From activation of fragments of the sulfur pellet, which were recovered from the floor, the total yield was estimated to be about  $6 \times 10^{16}$  fissions, which was supported by a temperature rise of over  $300^{\circ}\text{C}$  obtained by an extrapolation from the temperature record -- also off scale. It is interesting to note that this temperature rise is greater than the predicted limit of  $250^{\circ}$ , beyond which the tensile strength of the uranium should be exceeded, and the burst did indeed rupture the assembly.

Estimates based both on calculated internal pressures and the extent of damage, such as the telescoping of steel tubing, gave a value of 10 to 50 tons for the driving force which separated the components of the assembly. To put Godiva back into operation, it was necessary to machine the warped joining planes and repair the supporting framework. As mentioned in the preceding section, it was also necessary to add about a kilogram of uranium to attain a critical configuration because of the reactivity loss in warped parting planes and in small fissures near the center.

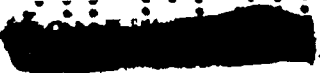
## CONCLUSIONS

Under prompt burst operation, the Godiva assembly is shown to be safe and simple to operate; the results are easily reproducible and can be satisfactorily explained by theory. Without danger of rupturing the active material, bursts with yields of  $2 \times 10^{16}$  fissions can be generated with a time duration of less than 100  $\mu\text{sec}$  (attained when bouncing of the upper section terminates fissioning). By exploiting the intense neutron flux associated with such a burst, one therefore can use such an assembly as an experimental tool for radiation pulsing. In fact, Godiva is so employed currently in activating fissile samples for measuring the delayed neutron periods and abundances.<sup>9</sup> The data presented in Table I were obtained by this means. Other possible uses for prompt bursts are in measurements of many short-lived activities, such as Sb-122 or 123 ( $n, \gamma$ ), and measurements on the delayed gammas from fission.

UNCLASSIFIED



UNCLASSIFIED

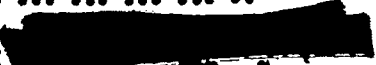

  
 0110

It was shown in the foregoing section that the shape of the trailing edge of weak bursts is extremely sensitive to short-period delayed neutrons. For example, it was shown that the difference between the two bursts of Fig. 15 can be due to the presence for the indoor burst of additional delayed neutrons in the millisecond region having a total relative abundance of only 0.015. Accordingly, it may be concluded from the excellent agreement between theory (with no short-lived groups) and experiment for the 320- $\mu$ sec (outdoor) burst as seen in Fig. 10, that the abundance of delayed neutrons in the period range from 1 to 10 msec is negligible for U-235 fission.

## REFERENCES

1. J. R. Dietrich and D. C. Layman, Argonne National Laboratory Report ANL-5211, Feb. (1954).
2. F. de Hoffmann, B. T. Feld, and P. R. Stein, Phys. Rev. 74, 1330 (1948).
3. K. Fuchs, Los Alamos Scientific Laboratory Report LA-596, Aug. 2, 1946.
4. G. E. Hansen, Los Alamos Scientific Laboratory Report LA-1441, July (1952).
5. See, for example, H. Hurwitz, Jr., Nucleonics 5, 61-67, July (1949).
6. J. D. Orndoff and C. W. Johnstone, Los Alamos Scientific Laboratory Report LA-744, Nov. 9, 1949.
7. R. E. Peterson and G. A. Newby, "Lady Godiva - An Unreflected U-235 Critical Assembly" (To be published in Nuclear Science and Engineering) and Los Alamos Scientific Laboratory Report LA-1614, Sept. (1953).
8. H. C. Paxton, Nucleonics 13, 48-50, October (1955).
9. G. R. Keepin and T. F. Wimett, "Delayed Neutrons" in Vol. 4 of Proceedings of the International Conference on the Peaceful Uses of Atomic Energy, 162-170, United Nations (1956).

UNCLASSIFIED


  
 0110